Modeling the Interactions Between Air Distribution Systems, Building Envelopes, and the Outdoor Environment in a Typical Hot, Humid Climate Residence

Lixing Gu, Ph.D., P.E. **Philip W. Fairey** **Muthusamy V. Swami, Ph.D.** **Jo Ellen Cummings**
Member ASHRAE

ABSTRACT

Air leakage and duct wall conduction in forced air distribution systems often waste 20% to 40% of the energy used to condition residences in hot, humid climates. The simulation of these forced air distribution system leakages, their attendant uncontrolled airflows within the building system, and their consequential energy uses may be achieved by treating building spaces as pressure vessels (nodes) that are interconnected with the forced air distribution system, the outdoors, and each other through the basic laws of pressure and airflow. A detailed, hourly building energy simulation program, subjected to rigorous analytical and theoretical evaluation and validated against high-quality, empirical data, is used in this study to simulate these complex interactions in a typical residence located in Miami, Florida.

Since energy uses related to forced air distribution systems are dependent on a number of factors, including duct system location and insulation level and the rate and location of the air leakage, a parametric simulation analysis that varies these factors across a range of typical values is used to conduct this investigation. The simulations quantify and disaggregate the typical residential energy uses for a peak summer day in Miami, Florida. The individual components of the predicted energy use that are related to the forced air distribution system include the duct wall conduction, the sensible and latent energy uses resulting from supply and return leaks, and the mechanically induced infiltration caused by the unbalanced forced air distribution system. Delivery and distribution efficiencies for the forced air systems on the peak summer day are calculated for each parametric case as compared with an ideal forced air system that experiences no air leakage and no duct wall conduction. By including accurate pressure and airflow models in the building simulation, the model can provide more accurate prediction. Simulation results show increased energy use in the typical Miami, Florida, residence by between 33% and 42%.

INTRODUCTION

Single-story, slab-on-grade concrete floor construction is the predominant residential construction practice in hot, humid climates. In such homes, the forced air distribution systems are usually located in attics and have been shown to waste 20% to 40% of the energy provided to condition typical residences (Cummings et al. 1991). Energy waste of this magnitude makes it imperative that the likely forced air leakage, duct wall conduction, and related uncontrolled airflows in such homes be thoroughly investigated and understood.

However, it is prohibitively expensive to develop an in-depth understanding of forced air distribution system impacts solely through field study. Detailed computer simulations offer an important and relatively inexpensive adjunct to field study that can provide in-depth understanding and insight on whole-building system performance and component interactions. Simulation of the energy impacts of forced air distribution systems may be achieved by treating the building space envelope as a complex network of pressure node vessels that are interconnected with each other, the forced air distribution system, and the outdoors through the basic laws of pressure and airflow. A detailed, hourly building energy simulation software program (FSEC 1992), subjected to rigorous analytical and theoretical evaluation (Gu et al. 1998a) and validated against high-quality, empirical data (Gu et al. 1998b), is used in this study to simulate these complex interactions in a typical residence located in Miami, Florida.

Lixing Gu is principal research engineer, **Philip W. Fairey** is deputy director, **Muthusamy V. Swami** is program director, and **Jo Ellen Cummings** is a research assistant at the Florida Solar Energy Center, Cocoa, Fla.

In actual buildings, forced air distribution system leaks interact with one another, the building envelope, the various pressure zones of the building, and the outdoor environment in complex, but understandable ways. In general, when the forced air distribution system supply leakage rate (normally to an attic) is larger than the return leakage rate (normally from a garage), the conditioned space is depressurized with respect to the outdoors. This negative pressure in the conditioned space causes outdoor air to infiltrate into the conditioned space through building envelope leaks. It also often causes the attic space (where the supply leaks normally occur) to be overpressurized with respect to the conditioned space, resulting in a flow of hot, humid attic air into the conditioned space through ceiling air leakage pathways. The impact on cooling energy use of this mechanically induced infiltration from the attic to the house is usually more significant than if the airflow were to come directly from outdoors. There are two reasons for this: (1) during air-conditioning operation, the attic air is usually hotter and more humid from moisture released from interior surfaces during daytime in summer than the outdoor air, and (2) the ceiling is typically more leaky than the exterior walls.

Conversely, when the return leakage rate is larger than the supply leakage rate, the conditioned space is usually pressurized with respect to the outdoors, resulting in the exfiltration of air from the conditioned space. However, any supply leak to an adjacent space (most often the attic) may still create an air pressure in the adjacent space that is positive with respect to the conditioned space. Under these conditions, the air in the adjacent space will flow into the conditioned space through pathways in the zone boundary. The amount of the airflow is dependent on both the pressure difference and the leakage area of the boundary between the zones.

In addition, even when the conditioned space is neutral with respect to the outdoors, it is still possible to create uncontrolled airflow between the conditioned space and an unconditioned space, such as a garage or an attic. This occurs when the pressure in the unconditioned space is higher than the pressure in the conditioned space. Uncontrolled airflows that cause these pressure imbalances result in more energy to maintain the conditioned space at desired conditions.

MODELING ASSUMPTIONS

Prototype Home Characteristics

Shown in Figure 1, the prototype house is a single-story L-shaped ranch-style house with an open living plan, slab-on-grade concrete floor, and 139 m^2 (1500 ft^2) of conditioned space. The garage area is 42.4 m^2 (456 ft^2) and attic volumes are 107 m^3 (3769 ft^3) over the living zone and 56.5 m^3 (1996 ft^3) over the garage. The attic areas are modeled as separate spaces with a plywood wall separating them. The house aspect ratio is 1:1.6 with the longer axis running east to west.

The exterior frame wall consists of 12.7 mm (½ in.) gypsum drywall on the inside, R-19 batt insulation, and 11 mm (7/16 in.) exterior siding with a solar adsorptance of 0.75 and a far-infrared emmisivity of 0.9. The roof is composed of 12.7 mm (½ in.) plywood exposed to the attic and 6.4 mm (1/4 in.) shingles on the exterior with solar adsorptance of 0.85 and emmisivity of 0.9. The roof slope is 5:12. The floor consists of 0.1 m (4 in.) concrete with 12.7 mm (½ in.) carpet on the interior. The ceiling is composed of 12.7 mm (½ in.) gypsum drywall and R-30 fiber glass insulation.

A constant natural infiltration rate of 0.35 ACH (air changes per hour) is assumed. The cooling thermostat set point is 25.6°C (78°F). The cooling equipment has a total airflow of 0.66 m^3/s (1400 cfm), a total cooling capacity of 3.5 tons, and a SEER of 10.0. All ducts in the system are insulated to a thermal resistance of R-4.2. The layout of the duct system is also shown in Figure 1.

Five zones are used in the building simulation: living zone, garage, garage-attic, lower living-attic air zone, and upper living-attic air zone. The two-zone living-attic air model accounts for detailed radiation, buoyancy, wind-driven airflows, and thermal stratification within the attic airspace (Parker et al. 1991). A single living-attic zone that combines the two attic thermal zones is used for airflow and pressure calculation. Miami TMY weather tape data were used and June 18 was chosen as the peak summer day for the simulation because the highest dry-bulb temperature occurs on this day. The maximum and minimum temperatures are 33.9°C and 23.9°C, respectively, with coincident relative humidities of 46% and 90%. The average temperature and relative humidity for this day are 28.5°C and 73%, respectively. An effective moisture penetration depth (EMPD) model (Keresteciogiu et al. 1990) was used to simulate wall moisture absorption and desorption. In order to eliminate the impact of initial conditions, four consecutive days were simulated, and results were reported for the fourth day.

Building Envelope Leakage Characteristics

The leakage characteristics of the building envelope are a critical determinant of the interactions between the forced air distribution system and the building spaces. For this study, an effort was made to define these characteristics to be as typical as possible. Field studies of 99 existing central Florida homes (Cummings et al. 1991) have shown average measured leakage of 12.7 ACH_{50} at an average floor area of 150 m^2 (1616 ft^2). Normalizing for floor area, a leakage of 11.8 ACH_{50} is obtained for the 139 m^2 (1500 ft^2) prototype home used in the study.

The air volume of the prototype house is 340 m^3 (12,000 ft^3). Thus, the equivalent airflow rate at 50 Pa is 1.114 m^3/s (2360 cfm). A power law formulation with a flow exponent of 0.65 is used to describe the relationship between airflow and pressure. Assuming 4 Pa as the standard reference pressure (Sherman et al. 1984), the effective leakage area (ELA) of the entire building shell is calculated to be 835 cm^2.

For the one-story prototype house with slab-on-grade floor, the portion of the building envelope subject to leakage consists of exterior walls, windows, doors, and ceiling. Leak

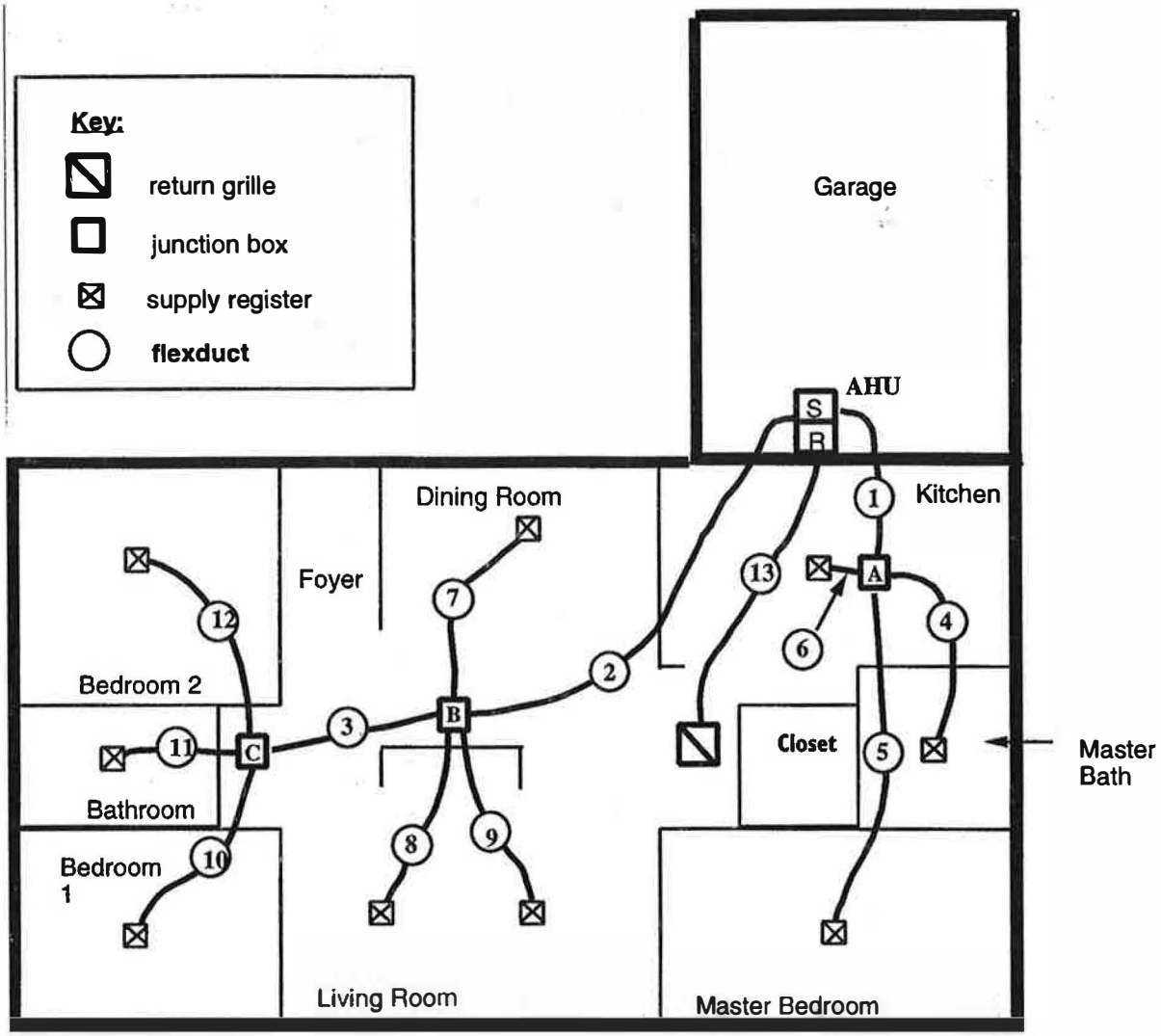

House Characteristics:

- **1500 sq. ft. (conditioned space)**
- **floor construction varies by climate**
- **frame walls with insulation level depending on climate**
- **ceiling insulation depends on climate**
- **224 sq. ft. windows equally distributed on each side of the house**
- **roof: hip gable, shingled, medium color no roof overhang**
- **duct construction and location depends on climate**
- **equipment capacity depends on climate**

Figure 1 *Prototype house floor plan and layout of air distribution system.*

age distribution for these components is assumed to be 30% for walls, 23% for windows and doors, and 47% for ceiling. Since windows and doors are subcomponents of the exterior walls, the exterior wall leakage areas are assumed to be the summation of the wall, window, and door leakage, yielding a total "wall" leakage area of 443 cm^2. This leakage area is applied over an effective "wall" area of 119 m^2, yielding a normalized "wall" leakage of 3.72 cm^2/m^2. Thus, the effective leakage area of the portion of the exterior "walls" separating the living space from the outdoors is 391 cm^2, and the effective leakage area of the portion separating the garage and the living area is 51.2 cm^2. The total and normalized effective leakage areas of the 139 m^2 ceiling are 393 cm^2 and 2.8 cm^2/m^2. The normalized ceiling leakage area in the prototype house is equivalent to the maximum effective leakage area of general ceilings, as listed in ASHRAE (1997). The effective leakage area in the building envelope was treated as an open area in the model (Swami et al 1992).

Using the minimum code attic ventilation requirement (SBCCI 1995) of 1.0 m^2 of net free ventilation area per 300 m^2 of attic floor area, the effective leakage areas between the living attic and outdoors and between the garage attic and outdoors are calculated to be 4630 cm^2 and 1400 cm^2, respectively. Based on roof area, a normalized effective leakage area for the attic is calculated as 27.8 cm^2/m^2. Assuming that the partition between the living attic and the garage attic has the same normalized effective leakage as the remainder of the attic and a "roof area" of 9.1 m^2, the effective leakage area between the two attic spaces is calculated as 252 cm^2.

Finally, assuming the garage exterior walls have the same normalized ELA as the exterior walls in the living area, the effective leakage area for the garage wall is 188 cm^2. The garage ceiling is treated in a similar manner, yielding an effective leakage area of 119 cm^2.

Table 1 summarizes the above discussion, providing the normalized and total effective leakage areas used by the simulation at the airflow interface boundaries.

Test Cases

Five test cases are used in the study as follows:

- Case 1 is an ideal duct system, with very high resistance (R-1000) duct insulation and no duct leakage. This case is used as the reference case to calculate distribution efficiency for the other four cases.
- Case 2 is designed with a single supply leak in the supply plenum that is leaking to the garage attic and a return leak into the return plenum that is leaking from the garage. The field research has determined that a supply leak of 5% of the total fan flow with a return leak of 10% of the total fan flow is the most common occurrence in existing Florida homes (Cummings et al. 1991). For this case, the supply leak to return ratio is approximately 0.5 (return dominant leakage).
- Case 3 is designed to have a supply leak from the junction box (A) to the living zone attic and a return leak from the garage. The supply leakage rate, however, is increased to be as large as the return leak such that the supply leak to return leak ratio is approximately 1.0 (balanced leakage).
- Case 4 is designed to have the same supply leak and return leak locations as Case 3 (Junction Box A) and living zone attic, respectively. However, the return leakage rate has been reduced to 5% of the total flow in this case and the supply leak to return leak ratio is approximately 2.0 (supply dominant leakage).
- Case 5 is designed to have the 10% return leak located immediately prior to the return plenum. The return leak airflow originates in the attic over the living space and is approximately twice the supply leakage air flow (5% of the total flow).

TABLE 1
Effective Leakage Areas Used for Simulations

Airflow Boundary	Normalized ELA (cm^2/m^2)	Component Area (m^2)	Total ELA (cm^2)
Living Area↔Outdoors	3.7	105.2	391.3
Living Area↔Garage	3.7	13.8	51.2
Living Area↔Living Attic	2.8	140.2	392.5
Garage↔Outdoors	3.7	50.5	188.0
Garage↔Garage Attic	2.8	42.5	119.0
Living Attic↔Outdoors	27.8	166.8	4630.0
Garage Attic↔Outdoors	27.8	50.5	1400.0
Garage Attic↔Living Attic	27.8	9.1	252.0

TABLE 2
Summary of Leakage and Mechanically Driven Infiltration for Cases 2-5

Case	Leak (%) Flow and Location				Mechanically Driven Infiltration (ACH)		
	Supply Flow (%)	To	Return Flow (%)	From	Ambient	Garage	Living Attic
2	5.00	Attic(G)	10.02	Garage	0	0	0
3	10.06	Attic(L)	10.00	Garage	0.036	0	0.068
4	10.00	Attic(L)	5.05	Garage	0.188	0	0.200
5	5.00	Attic(G)	10.04	Attic(L)	0	0	0

Duct leakage is modeled through the pressure-flow relationship, with an exponent of 0.65, between the duct and the buffer space connected by openings in the duct wall. A constant flow fan is used in the simulation.

RESULTS AND DISCUSSION

Simulation Procedure

The leakage areas are assumed to be a single opening area at airflow boundaries between spaces. Detailed information on modeling duct leakage and house performance can be found in Gu et al. (1996).

Pressures and Airflows

Table 2 summarizes the percent of supply and return duct leakages compared to the total fan flow. It also provides the mechanically induced infiltration rates resulting from the uncontrolled airflows. ACH (air change per hour) is calculated as the ratio of the uncontrolled airflow rate to the space air volume. Exfiltration (air leaving the conditioned space) is not included in the mechanically induced infiltration rates listed in Table 2.

Table 3 presents predicted pressures (in Pa with respect to outdoors) that are produced in each of the simulation zones as a result of equipment operation, excluding stack and wind impact. It is noted that the pressure distributions listed in Table 3 were calculated based on no indoor-outdoor air temperature difference or wind impact. As expected, the living area is pressurized for cases in which return leakage dominates and depressurized in cases where supply leakage dominates.

TABLE 3
Pressure Distributions During Equipment Operation (Pa)

Case	Living Area	Living Attic	Garage Attic	Garage
1	0	0	0	0
2	0.15	0	0	−2.26
3	−0.02	0.04	−0.04	−2.39
4	−0.27	0.03	−0.01	−0.88
5	0.22	−0.03	0.07	0.05

Case 2 corresponds to a 5.00% supply leak and a 10.02% return leak. Since the dominant return leak tends to pressurize the conditioned space, exfiltration occurs through the building envelope. The return leak depressurizes the garage, but the living attic is neutral because of the attic being very leaky and the supply leak being relatively small in comparison. The relatively large pressure differential between the garage and the garage-attic causes increased airflow from the garage attic to the garage.

Case 3 corresponds to a 10.06% supply leak and a 10.00% return leak. Although the supply leak in this case is just slightly larger than the return leak, it nonetheless causes a very slight negative pressure in the conditioned space. It creates 0.036 ACH infiltration from outdoors. In addition, due to pressurization, a living-attic 0.068 ACH of uncontrolled airflow from the living-attic to the conditioned space is predicted. The garage is again most depressurized.

Case 4 corresponds to a 10.00% supply leak and a 5.05% return leak. In this case, a net loss from the conditioned space through the dominant supply leak depressurizes the conditioned space, creating 0.1889 ACH infiltration from outdoors through the building envelope. Pressures in the zone where the supply leak terminates (living zone attic) and in the zone where the return leak originates (garage) are affected by the leaks even though these zones are very leaky. Greater pressure in the living-attic creates an additional 0.200 ACH of uncontrolled flow entering the conditioned space from the hot, humid attic.

Case 5 corresponds to a 5.00% supply leak to the garage attic and a 10.04% return leak originating from the living attic. Negative pressure due to the return leak is predicted in the attic over the living zone, and positive pressures are predicted in both the living area and in the attic over the garage where the supply leak terminates. Although the garage is pressurized with respect to the outdoors, it is depressurized with respect to the conditioned space, so there is an uncontrolled airflow from the conditioned space to the garage.

Hourly Simulation Result Plots

Figures 2, 3, and 4 show a detailed account of results of hourly simulations for cases 1, 4, and 5 respectively. These represent a combination of cases—where there is neither supply nor return leaks (Case 1, Figure 2), where the supply leak exceeds the return leak (Case 4, Figure 3), and where the return leak exceeds the supply leak (Case 5, Figure 4). Each figure is composed of six graphs. The first (a) and third (c) graphs present predicted daily temperature and relative humidity histories in the five zones of the house. The second (b) graph shows predicted sensible and latent loads removed by the equipment and the electrical energy use. The fourth (d) graph plots predicted duct wall conduction in the supply and return ducts during the equipment on-cycles (steady-state loss). The fifth (e) graph displays predicted duct system sensible and latent leakage penalties from the supply and return ducts. The sixth (f) graph shows the predicted mechanically induced infiltration penalties, which summarize all uncontrolled airflows into the conditioned space from adjacent zones and outdoors due to pressure imbalances.

Case 1 is assumed to have a perfect distribution system, bereft of leaks or losses. It has no duct conduction or leak penalties as well as no mechanically induced infiltration penalty associated with it. Graphs d, e, and f of Figure 2, which are empty, are shown only for completeness and have no relevance. The effect of supply and return leaks can be understood by cross-comparing each of the six graphs in Figures 2, 3, and 4.

Leaks negatively impact the energy used to condition a building in more ways than one. A supply leak is a direct loss of energy that could otherwise be used for conditioning the space and the loss is directly proportional to the leakage magnitude. Similarly, return leaks are an added burden on conditioning equipment and proportionately increase energy use. However, for the same leak percent, return leak impact is smaller than that of supply leaks (compare Figures 2e, 3e, and 4e).

Added penalty due to mechanically induced infiltration may occur due to imbalances between supply and return leaks. Supply leaks higher than return leaks will cause the room to be depressurized with respect to the ambient (and possibly with respect to the attic as well), drawing in additional hot air from the ambient and possibly the attic as well during the day. This penalty could be an additional 5% to 10% on the total load. Return leaks larger than supply leaks do not cause this additional penalty (compare Figures 2f, 3f, and 4f).

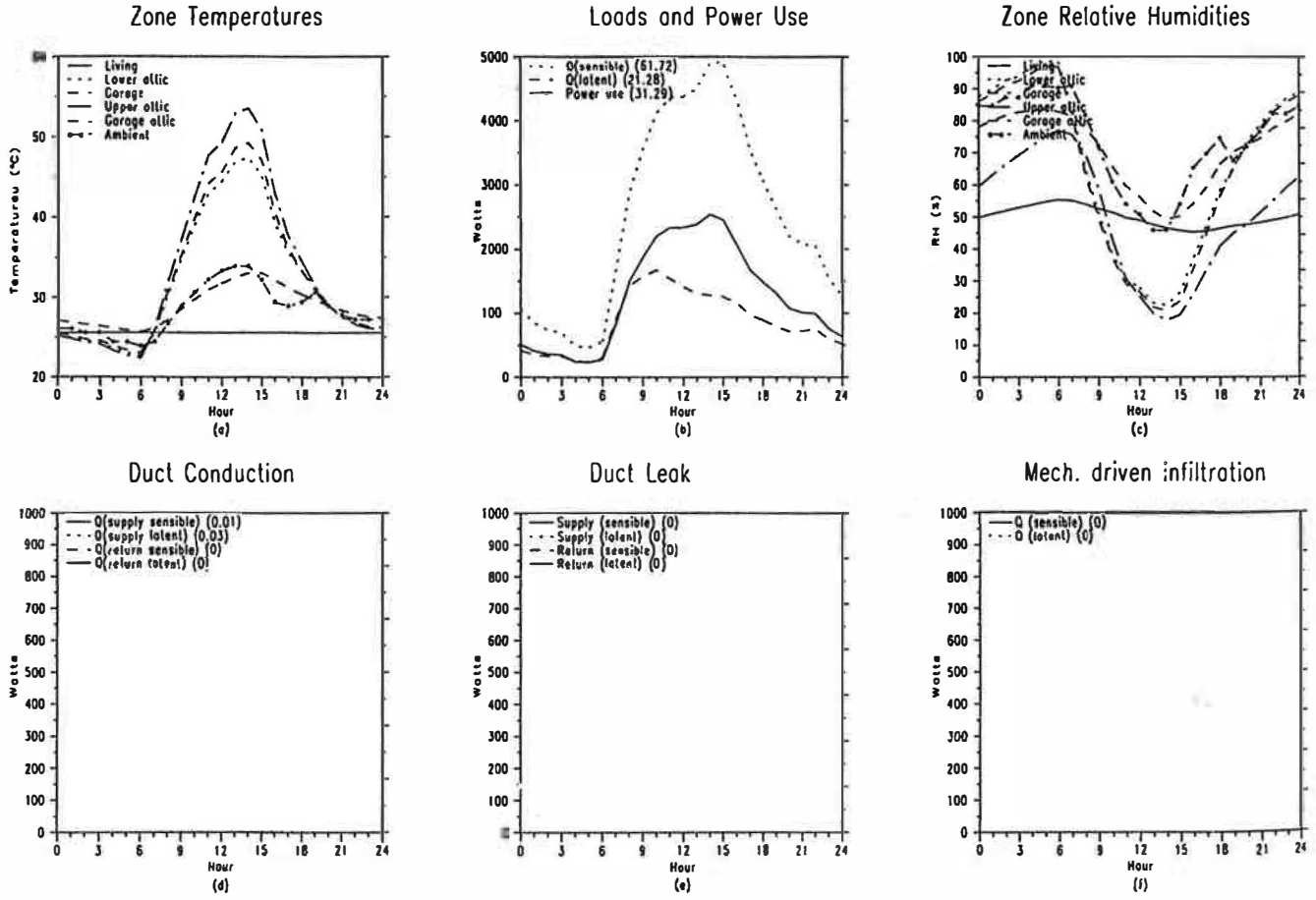

Figure 2 *House performance for a peak summer day in Miami (Case 1).*

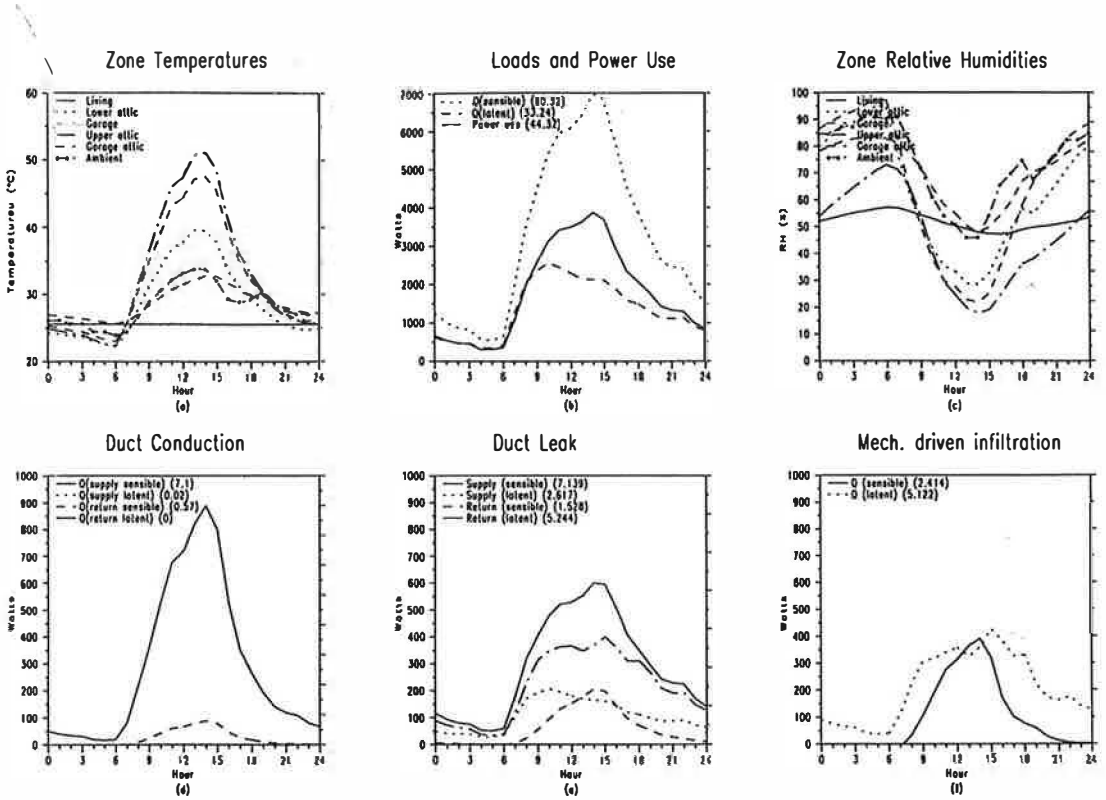

Figure 3 *House performance for a peak summer day in Miami (Case 4).*

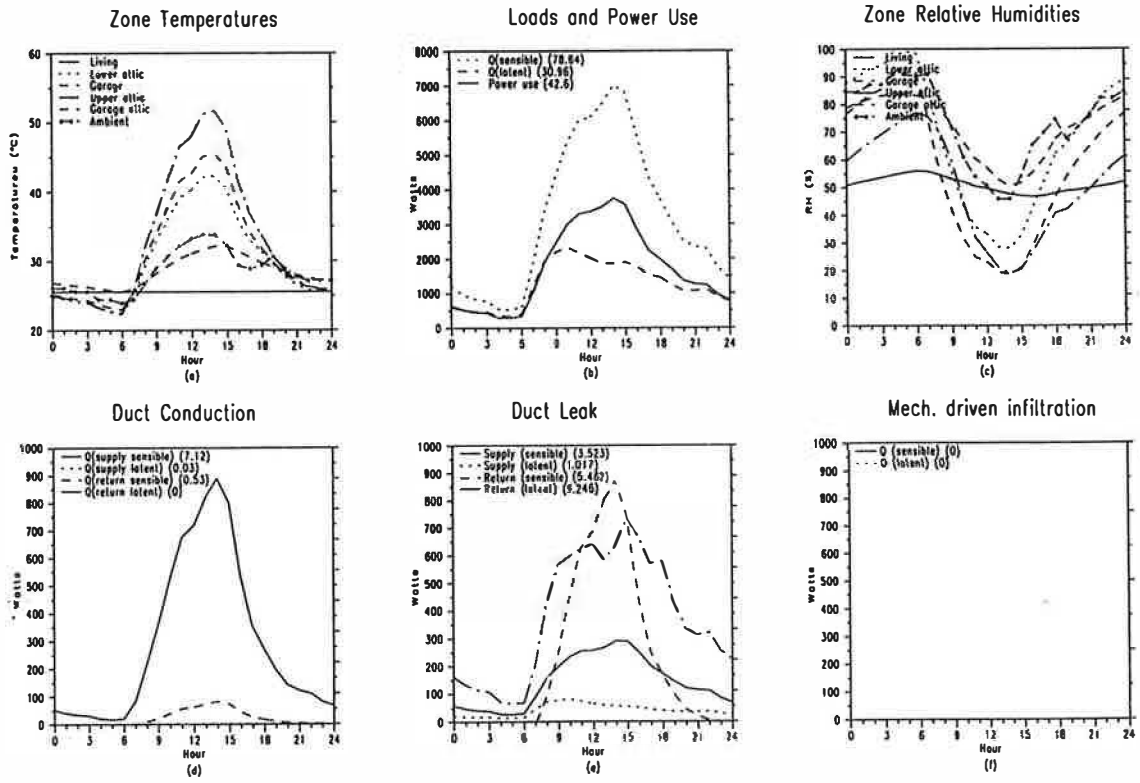

Figure 4 *House performance for a peak summer day in Miami (Case 5).*

The penalty due to a supply leak may be somewhat mitigated by its impact on the buffer space in which the leak occurs, whereby some of the energy lost is recouped by a process termed "regain." For the cases discussed in this paper, a supply leak into the attic tends to cool the attic space (compare Figures 2a, 3a, and 4a), which, in turn, tends to reduce the heat flow from the ceiling into the conditioned space and the conduction losses through the ducts. The reduction, however, depends on the insulation levels in the ceiling and ducts, and, for well-insulated ceilings and ducts, the "regain" could at best be marginal.

Conduction losses in the duct are primarily a function of the duct insulation and the temperature regimes in its surroundings. In the cases simulated, supply leaks into the attic space do not have any significant impact on the duct conduction losses (compare Figures 2d, 3d, and 4d).

The key point to be understood here is that the impact of leaks in distribution systems cannot be evaluated in isolation. Rather, their complex interaction with the building and

TABLE 4a
Component Loads and Penalties in a Peak Summer Day in Miami

Component	Case 1 (kWh)	Case 2 (kWh)	Case 3 (kWh)	Case 4 (kWh)	Case 5 (kWh)	Load
Sensible Load	61.72	76.13	79.69	80.32	78.64	Qs
Latent Load	21.28	30.84	33.87	33.24	30.96	Ql
Energy Use	31.29	41.63	44.14	44.32	42.60	P
Conduction Penalties						
On Cycle						
Supply Duct Sensible	0.01	7.15	6.96	7.10	7.12	D1
Supply Duct Latent	0.03	0.03	0.02	0.02	0.03	D2
Return Duct Sensible	0.00	0.53	0.56	0.57	0.53	D3
Return Duct Latent	0.00	0.00	0.00	0.00	0.00	D4
Off Cycle						
Supply Duct Sensible	0.00	0.93	0.80	0.80	0.91	Dsof
Return Duct Sensible	0.00	0.02	0.02	0.02	0.02	Drof
Leakage Penalties						
Supply Duct Sensible	0.00	3.53	6.98	7.14	3.52	D5
Supply Duct Latent	0.00	1.02	2.22	2.62	1.02	D6
Return Duct Sensible	0.00	2.81	2.86	1.53	5.46	D7
Return Duct Latent	0.00	8.93	9.51	5.24	9.25	D8
Mechanically Driven Infiltration						
Sensible Load	0.00	0.00	0.80	2.41	0.00	Is
Latent Load	0.00	0.00	1.59	5.12	0.00	Il
Wall Loads						
Buffer Space Heat Flow	5.09	4.56	4.13	4.14	4.49	Qf
Summary Results						
Total Load	83.00	106.97	113.56	113.56	109.60	Qt = Qs + Ql
Total Sensible Duct Penalty	0.01	14.97	18.18	17.16	17.56	Ds = D1+D3+Dsof+Drof+D5+D7
Total Latent Duct Penalty	0.03	9.98	11.75	7.88	10.30	Dl = D2+D4+D6+D8
Total Duct Penalty	0.04	24.95	29.93	25.04	27.86	Dt = Ds+Dl
Total Infiltration Load	0.00	0.00	2.39	7.53	0.00	It = Is+Il

TABLE 4b
Component Penalties in a Peak Summer Day in Miami

Component	Case 2 (%)	Case 3 (%)	Case 4 (%)	Case 5 (%)	(%)
Sensible					
Conduction	11.34	10.47	10.57	10.91	(D1+D3+Dsof+Drof)/Qs
Leakage	8.33	12.35	10.79	11.42	(D5+D7)/Qs
Mechanically Driven Infiltration Load	0.00	1.00	3.00	0.00	Is/Qs
Total Sensible Penalty	19.66	23.82	24.37	22.33	(D1+D3+Dsof+Drof+D5+D7+Is)/Qs
Latent					
Conduction	0.10	0.06	0.06	0.10	(D2+D4)/QI
Leakage	32.26	34.63	23.65	33.17	(D6+D8)/QI
Mechanically Driven Infiltration Load	0.00	4.69	15.40	0.00	II/QI
Total Latent Penalty	32.36	39.39	39.11	33.27	(D2+D4+D6+D8+II)/QI
Sensible Plus Latent Penalty					
Conduction	8.10	7.36	7.49	7.86	(D1+D2+D3+D4+Dsof+Drof)/Qt
Leakage	15.23	18.99	14.56	17.56	(D5+D6+D7+D8)/Qt
Mechanically Driven Infiltration Load	0.00	2.10	6.63	0.00	It/Qt
Total Penalty	23.32	28.46	28.68	25.42	(D1+D2+...+Dsof+srof+D8+It)/Qt

system, such as interaction of pressure regimes, resulting airflows across building subsystems, buffer zone influences, equipment performance impacts, etc., must be carefully considered to fully understand and evaluate their impact on energy use.

Duct System Energy Penalties

Table 4a provides all component loads and penalties for each of the five cases. The rightmost column indicates how these items are calculated. It should be pointed out that the duct conductive energy loss is composed of steady-state and transient losses. The cooling equipment cycles on and off several times during each hour. The steady-state loss represents duct energy loss during the equipment on-cycles, while the transient loss represents extra energy needed to remove heat that is gained and stored during the equipment off-cycle. Table 4b presents component penalties as a percent of total sensible and latent loads. Again, the rightmost column indicates how these percentages are calculated with the symbols referring back to the values presented in Table 4a. Table 4c gives delivery and distribution efficiencies with respect to total loads and power consumption. Three different delivery

TABLE 4c
Delivery and Distribution Efficiencies in a Peak Summer Day in Miami

	Case 2 (%)	Case 3 (%)	Case4 (%)	Case 5 (%)	(%)
Delivery Efficiency					
Sensible	80.34	77.19	78.64	77.67	(1-Ds/Qs)
Latent	67.64	65.31	76.29	66.73	(1-DI/QI)
Total Delivery Efficiency	76.68	73.64	77.95	74.58	(1-Dt/Qt)
Distribution Efficiency					
Sensible	81.07	77.45	76.84	78.48	(Qsi/Qs)
Latent	69.00	62.83	64.02	68.73	(QIi/QI)
Total Distribution Efficiency	77.59	73.09	73.09	75.73	(Qti/Qt)
Heat Regain					
Buffer Space Regain Factor	0.90	0.81	0.81	0.88	(Qf/Qfi)

and distribution efficiencies are reported in the tables as follows: (1) sensible, (2) latent, and (3) total (sum of sensible and latent). Delivery efficiency is defined as the ratio between the energy supplied to the conditioned space compared with the energy entering the distribution system at the equipment heat exchanger. The distribution efficiency is the ratio between the energy consumption with and without the distribution system. Sensible and latent distribution efficiencies and heat regain from the buffer space are based on simulation results from Case 1.

GENERAL CASE ANALYSIS

Case 2

In this case, the conditioned space is pressurized due to a dominant return leak from the garage. Because the conditioned space is pressurized, there is no mechanically driven infiltration. Since the supply leak terminates in the garage attic, it makes the garage attic cooler. Because the garage attic is very leaky to the outdoors and only partially open to the living attic, the supply leak does not cause an airflow from the garage attic to the living attic. However, the duct wall conduction in the living attic makes the living attic cooler, and, as a result, the ceiling heat gain is reduced by about 10% compared to the ideal duct case (Case 1).

In addition to the amount of leakage, the location of the duct leakage is also important. The nearer the leak is to the equipment heat exchanger, the more leakage penalty is expected. This occurs because the conditioned air near the heat exchanger is colder than the air far away due to duct wall conduction.

Peak day delivery efficiencies for sensible, latent, and total loads are 80.3%, 67.6%, and 76.7%, respectively. Peak day distribution efficiencies for sensible, latent, and total loads are 81.1%, 69.0%, and 77.6%, respectively. (Distribution efficiency is often higher than the delivery efficiency due to buffer space regain—in this case caused by the impact of the reduced attic air temperature on ceiling heat gain.) It should be pointed out that latent loads play an important role when the efficiency is calculated, especially for return-dominated leakage in hot, humid climates such as Miami. This case vividly illustrates this principle, and the latent delivery and distribution efficiencies are significantly lower than the sensible efficiencies as a result.

Case 3

The amount of supply leak in this case is double that of Case 2, but the return leakage rate remains almost identical to Case 2. The supply leakage flows into the living attic and is slightly greater than the return leakage flow from the garage. This relatively large supply leak pressurizes the living attic zone with respect to the outdoors, the garage attic zone, and the living zone. The garage zone is significantly depressurized. Uncontrolled airflows into the depressurized garage are the reason for the depressurization of the living zone and garage attic zone with respect to the outdoors. Peak day delivery efficiencies for sensible, latent, and total are 77.2%, 65.3%, and 73.6%, respectively. Peak day distribution efficiencies are 77.5%, 62.8%, and 73.1%. In this case, distribution efficiencies are lower than delivery efficiencies. Depressurization of the conditioned space with respect to the living attic forces uncontrolled airflow from the attic to the conditioned space, completely overcoming the buffer space regain due to the reduction in ceiling heat gain.

Case 4

This case is designed with the same supply leakage rate and leak site locations as Case 3. However, the return leak is reduced to 5% of the fan flow. Thus, the supply leak is dominant and the conditioned space is much more depressurized than in Case 3. Significantly more mechanically induced infiltration from the living-attic enters the conditioned space due to the greater pressure difference between the living-attic and the conditioned space. At the same time, outdoor air is also drawn into the conditioned space. Peak day delivery efficiencies for sensible, latent, and total are 78.6%, 76.3%, and 78.0%, respectively, and distribution efficiencies are 76.8%, 64.0%, and 73.1%. Since the return leak is decreased by almost half, this case yields higher delivery efficiencies than Case 3, but because the mechanically induced infiltration is quite large, the total distribution efficiency is virtually the same as in Case 3.

Case 5

The return leak for this case originates in the living-attic zone and the supply leak terminates in the garage-attic zone. Since the return leak is larger than the supply leak, the living-attic is depressurized. The dominant return leak pressurizes the living zone, and there is no mechanically driven infiltration flowing into the conditioned space. Sensible, latent, and total delivery efficiencies are 77.7%, 66.7%, and 74.6%, while distribution efficiencies are 78.5%, 68.7%, and 75.7%, respectively. Since there is some buffer space regain and no mechanically driven infiltration, the delivery efficiency is lower than the distribution efficiency.

COMPARATIVE EXAMINATION

Load and Power Consumption

Figure 5 shows sensible and latent loads and power consumption for all cases simulated. Excluding case 1, which is the reference, a comparison between cases 2 through 5 indicates the following:

	Highest (kWh)	**Lowest** (kWh)
Sensible Load	80.32, Case 4	76.13, Case 2
Latent Load	33.87, Case 3	30.84, Case 2
Energy Use	44.32, Case 4	41.63, Case 2

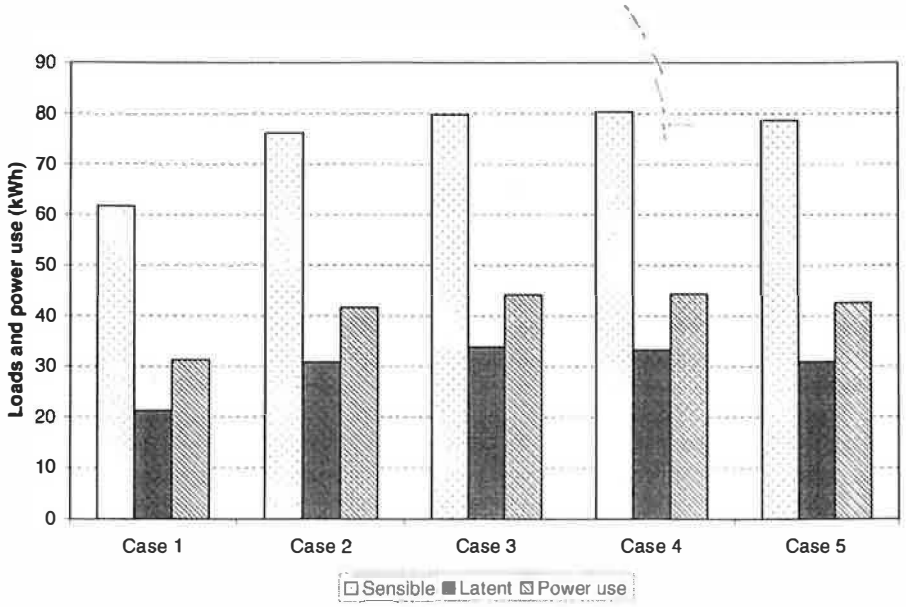

Figure 5 *Loads and energy demand on a peak summer day in Miami.*

Although from Figure 5, it appears that cases 3, 4, and 5 have similar total loads and energy use, a closer examination of Table 4 for these cases would disclose that component loads that contribute to the totals are not similar. For the cases simulated, it is apparent that the sensible load and power consumption correlate to the amount of mechanically induced infiltration. The living space is most depressurized and, therefore, draws more air from both the adjacent zones as well as the outdoors. The latent load, on the other hand, also appears to be tied to the return leak amount and source. Although it does increase with increasing supply leak, as is obvious, a return leak from the attic has a greater impact than one from the garage. These results appear very consistent with leakage and infiltration results listed in Table 2.

Figure 6 presents percentage increases in sensible and latent loads and energy consumption as compared to the corresponding loads of Case 1. The range of the calculated values are given below.

	Highest	**Lowest**
% increase in Sensible Load	30%, Case 4	23%, Case 2
% increase in Latent Load	59%, Case 3	44%, Case 2
% increase in Energy Use	42%, Case 4	33% Case 2

Note that Case 2 has the lowest increases in loads and energy use and is typical of homes found in Florida. Although the supply and return leak combination does not produce any mechanically induced infiltration, yet it requires an additional 33% in cooling energy just to over-

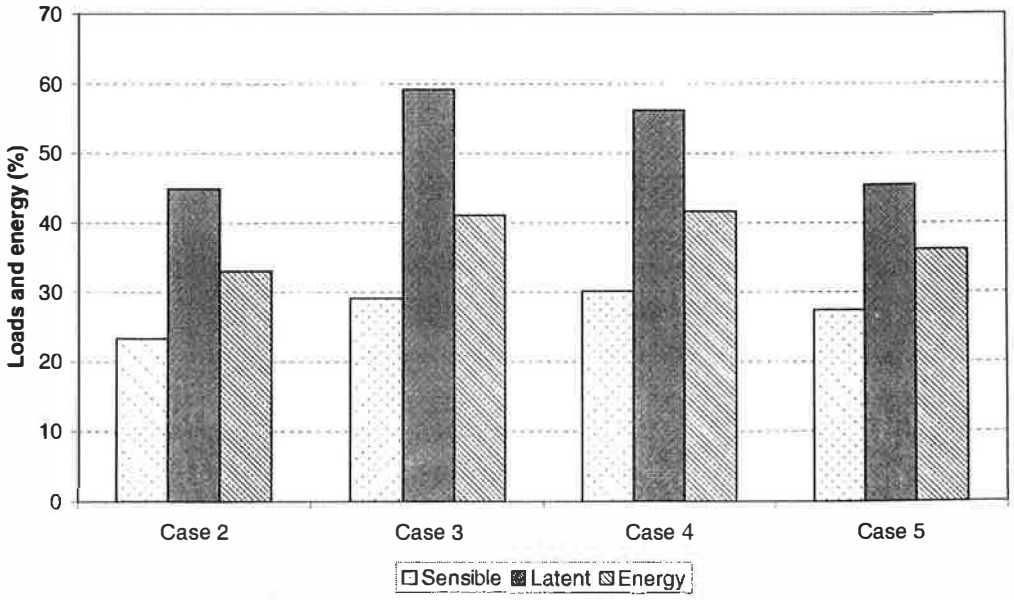

Figure 6 *Percentage increase of loads and energy demand on a peak summer day in Miami.*

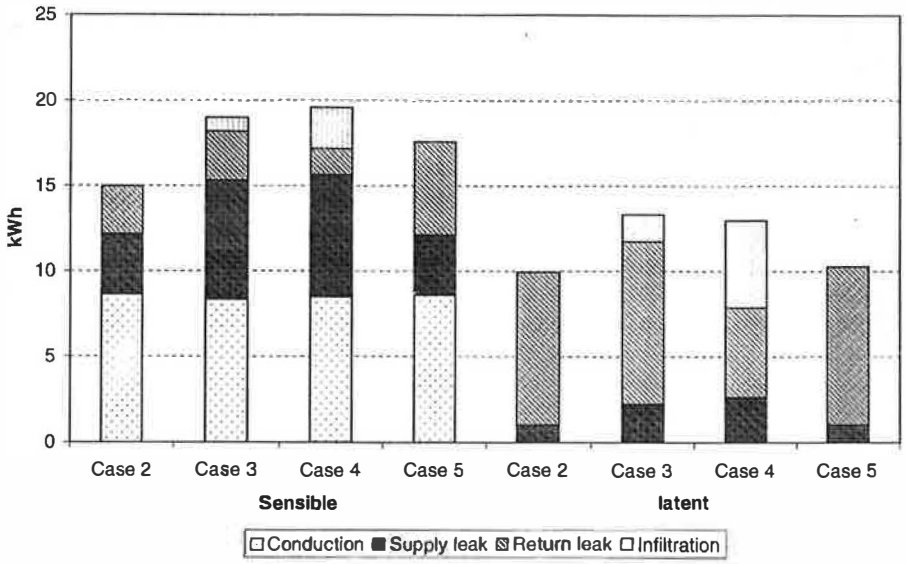

Figure 7 *Duct system energy loss on a peak summer day in Miami.*

come duct system penalty when compared to the reference case (Case 1). With conditions where mechanically induced infiltration occur, such as in Case 4, the penalties can only worsen.

Duct Conduction Energy Losses

Figures 7 and 8 show duct component energy losses for Cases 2 through 5. These losses include both steady-state and transient components indicated in previous tables. Case 1 is not included because there are no penalties associated with the distribution system. Figure 7 presents the actual kWh values, while Figure 8 presents them as percentages of the total load. The conduction losses are fairly similar (around 8 kWh) for all the cases, varying only minimally among them, thereby indicating that it is most dependent on the duct insulation R-value, which has not been varied in this study. Considering the fact that supply leak configurations in cases 3 and 4 reduce attic air temperatures, it may be argued that the conduction losses in these cases must be significantly lower. While this is true for the rate at which heat is lost from the ducts, one must consider that increased supply leaks also cause a corresponding increase in equipment run times to meet the load and, consequently, would increase the total heat flow from the ducts. The net effect in the cases simulated in this study seems to keep the duct conduction losses similar. The percentages, however, show slightly more variation (7.3%

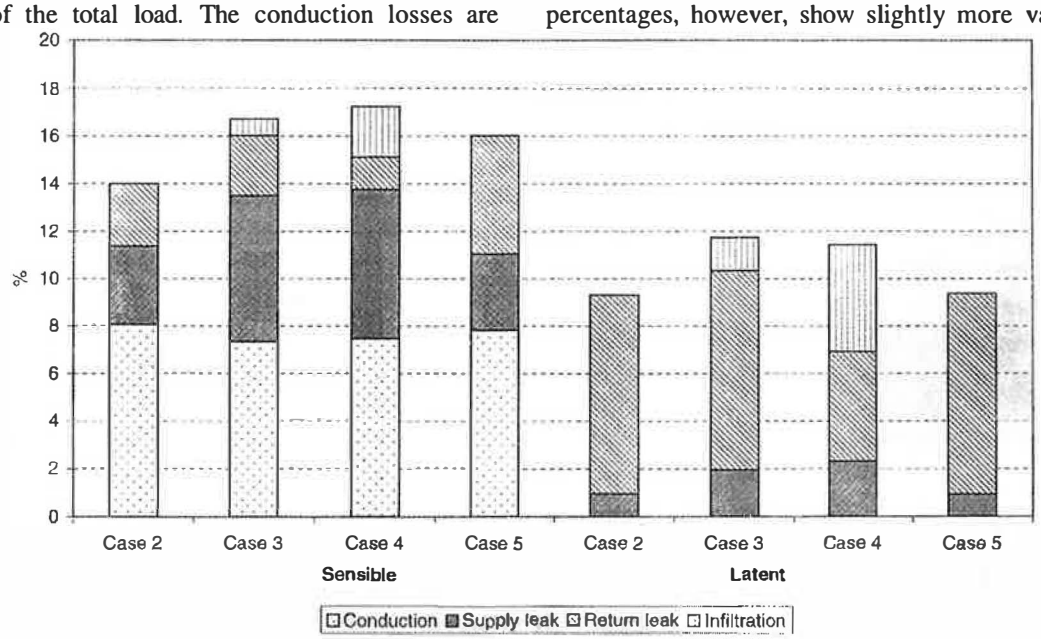

Figure 8 *Percentage of duct system energy losses on a peak summer day in Miami.*

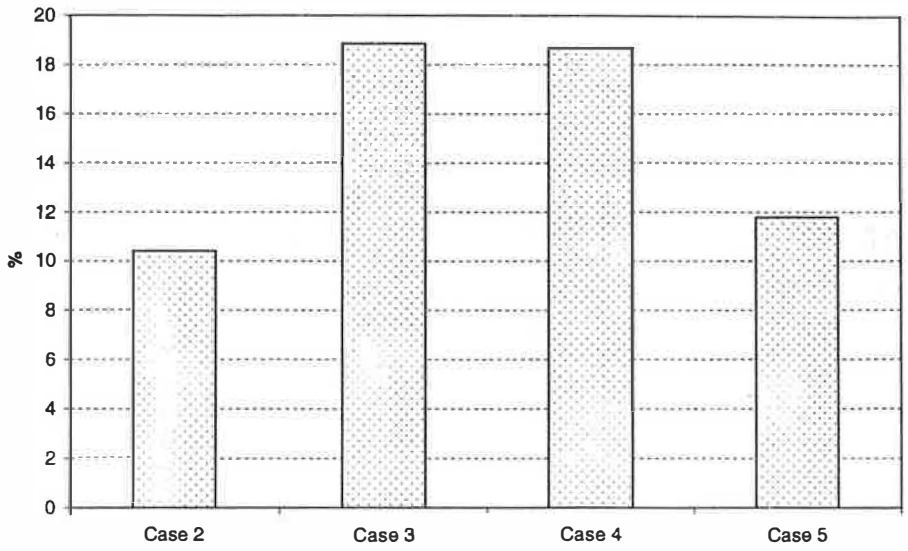

Figure 9 *Percent reduction of ceiling heat flux on a peak summer day in Miami.*

in case 3 to 8.1% in case 2) because it is calculated based on the total load.

Duct Leakage Energy Losses

Penalties associated with leakage are directly related to the leakage amounts and location. The range of penalties are summarized below both as raw kWh numbers and percentages of total load.

	Highest	Lowest
Supply leak sensible	7.14 (6.3%), Case 4	3.52 (3.3%), Case 5
Supply leak latent	2.62 (2.3%), Case 4	1.02 (0.9%), Case 5
Return leak sensible	5.46 (5%), Case 5	1.53 (1.4%), Case 4
Return leak latent	9.51 (8.4%), Case 3	5.24 (4.6%), Case 4

Examination of the above summary and Figures 7 and 8 shows that latent penalties are about half of the corresponding sensible penalties for supply leaks and about twice for return leaks. In raw kWh, return leaks have more impact on the latent load, while supply leaks have more impact on the sensible. load. Supply leak penalties are more dependent on leak amount and less on leak location, while for return leaks both the amount of leak and the location are important.

Mechanically Induced Infiltration

Mechanically induced infiltration occurs when a conditioned zone is depressurized with respect to adjacent zones or the outdoors. Cases 1, 2, and 5 have no mechanically induced infiltration penalties because the conditioned space is pressurized, while in cases 3 and 4, where the conditioned space is depressurized, these penalties exist, as given below for these two cases along with the conditioned space pressures.

Mechanically Induced Infiltration Penalties	**Case 3 (–0.02 Pa)**	**Case 4 (–0.27 Pa)**
	(kWh)	**(kWh)**
Sensible	0.8 (0.7%)	2.41 (2.1%)
Latent	1.59 (1.4%)	5.12 (4.5%)

These penalties are a direct result of pressure regimes caused by imbalances in supply and return leaks designated by the supply-to-return leak ratio. A value greater than one for this term will almost always cause depressurization in the conditioned space, leading to mechanically induced infiltration as in case 4. It is worth noting (see Table 2) that although the amount of mechanically induced infiltration airflow from the ambient and attic are comparable in case 4, their penalty contributions are not. Air drawn from a hot and humid attic is much more detrimental than air drawn in from outdoors.

Heat Regain Through Buffer Zone

Regain is defined as the portion of the energy lost by the distribution system that is recovered by the conditioned space. In the present study, regain is the reduction in ceiling flux (with respect to the reference case, case 1) brought about by reduced attic air temperatures. Figure 9 shows the ceiling heat flux reductions for Cases 2 through 5.

Delivery and Distribution Efficiencies

Figure 10 shows delivery and distribution efficiencies for Cases 2-5. Although separate sensible and latent efficiencies

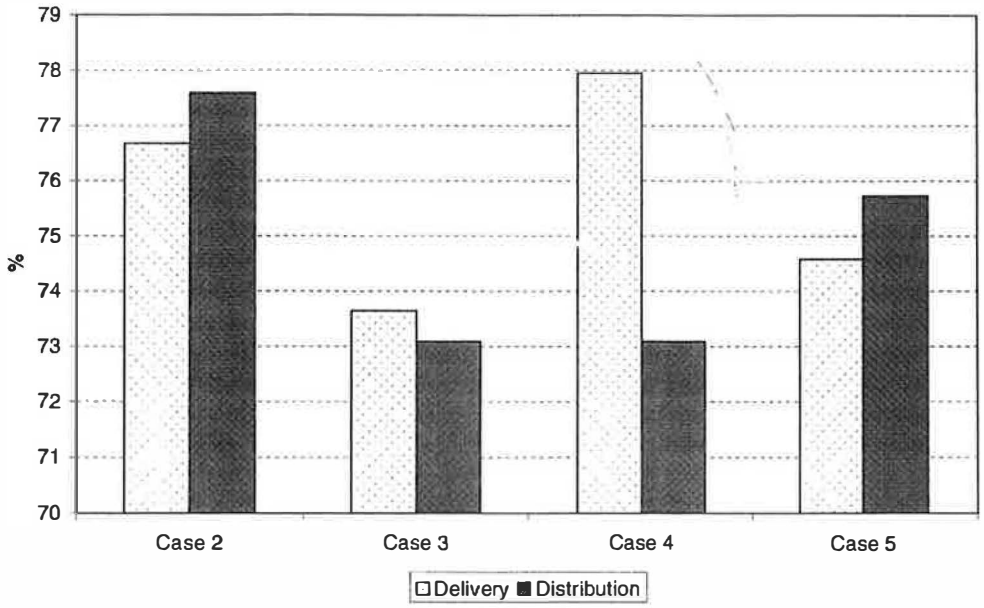

***Figure 10** Delivery and distribution efficiencies on a peak day in Miami.*

were given in earlier tables, only the efficiencies based on the total load (sensible + latent) are presented here. These efficiencies are important parameters that indicate how efficiently the system is performing. Shown below are the delivery and distribution efficiencies for cases 2 through 5, ordered from the lowest to highest delivery efficiencies.

Del. Eff.	Case No.	Dis. Eff.	Sup-L	Ret-L
73.64	Case 3	73.09	10%	10%
74.58	Case 5	75.73	5%	10%
76.68	Case 2	77.59	5%	10%
77.95	Case 4	73.09	10%	5%

Delivery efficiencies include the effect of conduction and leakage losses and are directly dependent on them—such as leakage amounts and duct R-value. Higher supply leakages result in lower delivery efficiencies for the same return leak. The distribution efficiency, however, gives a more accurate picture of the distribution system performance compared to an ideal system and includes all interactions. Under normal conditions, the distribution efficiencies are expected to be higher than delivery efficiencies because of the inclusion of regain in the former. This is true for cases 2 and 5, as seen above. However, for cases 3 and 4, the distribution efficiencies are lower than the delivery efficiencies. The difference between these two sets of cases is that for cases 2 and 5 there are no penalties associated with mechanically induced infiltration, whereas for cases 3 and 4 these penalties exist. The same data as listed above are presented below after ordering by distribution efficiency.

Dist. Eff.	Case No.	Del. Eff.	M-I Infl.
73.09	Case 3	73.64	2.24
73.09	Case 4	77.95	7.53
75.73	Case 5	74.58	0
77.59	Case 2	76.68	0

The distribution efficiencies are higher when mechanically induced infiltration is absent (Cases 2 and 5). When mechanically induced infiltration is present, the distribution efficiencies are lower (cases 3 and 4). Note that for cases 3 and 4, although the mechanically induced infiltrations are quite different, their distribution efficiencies are the same. The distribution efficiency represents other interactive effects not considered in the calculation of delivery efficiency. For cases 3 and 4, we may note that the differences between the delivery and distribution efficiencies (0.5% for case 3 and 4.8% for case 4) show the impact of and are directly related to the mechanically induced infiltration penalty.

CONCLUSIONS AND RECOMMENDATIONS

The following conclusions may be drawn from the above discussion.

- Predictions due to duct leak are proportional to the amount of leak. In general, supply leaks penalize sensible loads, while return leaks penalize latent loads. However, if the source of the return leak is hot and humid, such as an attic, it can make a significant contribution to the sensible load.
- In a hot, humid climate, mechanically driven infiltration generally trends to increase latent loads. In the absence of return leaks, when supply leaks pressurize attic zones and depressurize conditioned spaces, the resulting mechanically driven infiltration could come almost entirely from the attic instead of the ambient. This is especially true for slab-on-grade construction. Even though the amount of mechanically driven infiltration from the attic and outdoors may be comparable, as in the present study, the resulting energy penalties are quite different. The attic contributes a significantly larger penalty for the same amount of air. Therefore, reducing

leakages in the ceiling is much more important than increasing wall airtightness.

- Comparatively, the amount of the heat regain from buffer zones, such as the attic in the present study, may be far outweighed by energy penalties due to increased mechanically driven infiltration when the attic is more pressurized with respect to the conditioned space.
- Return leaks from a hot, humid source could result in significantly more latent energy penalties than sensible penalties resulting from supply leaks.
- The delivery efficiency by itself may not provide an accurate picture of duct system penalties. However, the distribution efficiency, which accounts for all interactive effects, does provide a more accurate picture of duct system penalties. This is because it compares a house with an actual duct system to the same house with an ideal duct system.

Energy loss in ducts could be a considerable portion of the total energy used to condition the living space. Cases examined in the present study indicate energy demand could be 33% to 42% more because of duct system inefficiencies. Building simulation tools, therefore, should endeavor to deal with the complex interactions of the air distribution system, building components, and outdoor environment in order to accurately predict building energy use.

REFERENCES

ASHRAE. 1997. *1997 ASHRAE Handbook—fundamentals*, Table 3, p. 25.16. Atlanta: American Society of Heating, Refrigerating and Air-Conditioning Engineers, Inc.

Cummings, J.B., J.J. Tooley, and N. Moyer. 1991. Investigation of air distribution system leakage and its impact in central Florida homes. FSEC-CR-397-91, Florida Solar Energy Center, Cape Canaveral.

FSEC. 1992. *FSEC 3.0, Florida software for environmental computation*. FSEC-GP-47-92, Florida Solar Energy Center.

Gu, L., J.E. Cummings, M.V. Swami, P.W. Fairey, and S. Awwad. 1996. Comparison of duct system computer models that could provide input to the thermal distribution standard method of test (SPC152P). FSEC-CR-926-96, Florida Solar Energy Center.

Gu, L., J.E. Cummings, M.V. Swami, and P.W. Fairey. 1998a. Comparison of duct system computer models that could provide input to the thermal distribution standard method of test (SPC152P). *ASHRAE Transactions* 104 (1).

Gu, L., M.V. Swami, J.E. Cummings, P.W. Fairey, T. Petrie, and J. Christian. 1998b. Comparison of a duct system computer model with measured data in a residential attic with a duct system. *ASHRAE Transactions* 104 (2).

Keresteciogiu, A., M. Swami, and A. Kamel. 1990. Theoretical and computational investigation of simultaneous heat and moisture transfer in buildings: Effective moisture penetration depth theory. *ASHRAE Transactions* 96 (1).

Parker, D., P.W. Fairey, and L. Gu. 1991. *A stratified air model for simulation of attic thermal performance. Insulation materials: Testing and applications*, Vol. 2, ASTM STP 1116, pp. 44-69. Philadelphia: American Society for Testing and Materials.

Sherman, M.H., D.J. Wilson, and D.E. Kiel. 1984. *Variability in residential air leakage. Measure Air Leakage of Building,* ASTM STP 904, H.R. Trechsel and P.L. Lagus, eds., pp. 349-364. Philadelphia: American Society for Testing and Materials.

SBCCI. 1995. *Standard building code.* Southern Building Code Congress International, Inc.

Swami, M.V., L. Gu, and V. Vasanth. 1992. Integration of radon and energy models for building. FSEC-CR-553-92, Florida Solar Energy Center, Cocoa, Fla.